Chinese Journal of Natural Medicines

New meroterpenoids featuring a rare 3/5/6/6/11/6/6 fused–ring skeleton from *Penicillium brefeldianum* SMU03 and their antifibrotic activities

Xia Cheng, Lei Di, Luying Wu, Qi Luo

Citation: Xia Cheng, Lei Di, Luying Wu, Qi Luo, New meroterpenoids featuring a rare 3/5/6/6/11/6/6 fused–ring skeleton from *Penicillium brefeldianum* SMU03 and their antifibrotic activities, Chinese Journal of Natural Medicines, 2026, 24(1), 112–118. doi: 10.1016/S1875–5364(26)61081–3.

View online: https://doi.org/10.1016/S1875–5364(26)61081–3

Chinese Journal of Natural Medicines 24 (2026) 112-118

Contents lists available at ScienceDirect

Chinese Journal of Natural Medicines

journal homepage: www.cjnmcpu.com/

Original article

New meroterpenoids featuring a rare 3/5/6/6/11/6/6 fused-ring skeleton from *Penicillium brefeldianum* SMU03 and their antifibrotic activities

Xia Cheng[a,b,Δ], Lei Di[c,Δ], Luying Wu[b], Qi Luo[b,*]

[a] *Guangzhou Municipal and Guangdong Provincial Key Laboratory of Molecular Target & Clinical Pharmacology, the NMPA and State Key Laboratory of Respiratory Disease, School of Pharmaceutical Sciences, Guangzhou Medical University, Guangzhou 511436, China*

[b] *Guangdong Provincial Key Laboratory of Chinese Medicine Pharmaceutics, School of Traditional Chinese Medicine, Southern Medical University, Guangzhou 510515, China*

[c] *Inflammation and Immune Mediated Diseases Laboratory of Anhui Province, School of Pharmacy, Anhui Medical University, Hefei 230032, China*

ARTICLE INFO

Article history:
Received 29 April 2025
Revised 16 July 2025
Accepted 5 September 2025
Available online 20 January 2026

Keywords:
Penicillium brefeldianum SMU03
Meroterpenoid
Antifibrotic activity
Plausible biosynthetic pathway

ABSTRACT

Penicine A (**1**), a meroterpenoid featuring a novel 3/5/6/6/11/6/6 polycyclic backbone, together with two new metabolites, penicines B (**2**) and C (**4**), and six known compounds, were isolated from the mangrove rhizosphere soil-derived fungus *Penicillium brefeldianum* SMU03. The structures of these metabolites were elucidated through extensive spectroscopic analysis combined with quantum chemical calculations. Notably, **1** exhibits a highly unusual molecular architecture, incorporating a dioxaspiro[4.5]decane motif and a rare bridgehead double bond (anti-Bredt system). A plausible biosynthetic pathway, involving sequential intermolecular [4 + 2] cycloaddition reactions, is proposed. Additionally, meroterpenoids **1** and **3** demonstrate significant antifibrotic activity in transforming growth factor β1 (TGF-β1)-induced human renal proximal tubular epithelial cells.

1. Introduction

The genus of *Penicillium*, one of the most prevalent fungi found in air, sea, soil, and various organisms, has a significant economic impact on human life [1, 2]. This genus is known to produce numerous secondary metabolites (over 1300 compounds), including alkaloids (notably the drug penicillin), polyketides, nonribosomal peptides, cyclic terpenoids, and hybrid compounds [1, 2]. Their remarkable and broad-spectrum bioactivities, including antifibrotic, anti-bacterial, anti-insect, anti-viral, anti-tumor, and cardiovascular effects, have garnered substantial attention from natural product researchers, synthetic chemists, and biochemists [3]. Kidney fibrosis represents a critical medical condition that can lead to severe complications and mortality [4]. Currently, no effective treatment exists for kidney fibrosis, making the search for novel therapeutic agents crucial. In recent years, our research team has focused on discovering and understanding novel small molecules that combat renal fibrosis, reporting several secondary metabolites with significant anti-renal fibrosis activity, including lingzhiol [4], applanatumin A [5], and sinensilactam A [5]. These promising small molecules encourage further investigation into natural products.

The fungus *Penicillium brefeldianum* was isolated from mangrove soil collected at Wetland Parks of Huiyang, Guangzhou, China. Chemical investigation of this strain's secondary metabolites yielded a novel meroterpenoid with a distinctive 3/5/6/6/11/6/6 polycyclic backbone, penicine A (**1**) (Fig. 1), alongside the known meroterpenoid pughiinin A (**3**) [6]. Additionally, the study identified a new sesquiterpenoid (**2**), two alkaloids (**4** and **7**), three polyketides (**5**, **6**, and **8**), and a terphenyl compound (**9**). The antifibrotic activity of compounds **1**–**9** was evaluated in transforming growth factor β1 (TGF-β1)-induced human renal proximal tubular epithelial cells (HK-2). The biosynthesis pathway of **1**, involving two consecutive hetero-Diels-Alder reactions, is briefly discussed.

2. Results and discussion

Penicine A (**1**), isolated as a white powder, was determined to have the molecular formula $C_{32}H_{40}O_8$ through high-resolution electrospray ionization mass spectrometry (HR-ESI-MS) (*m/z* 553.2796 $[M + H]^+$) with 13 degrees of unsaturation. The ^1H nuclear magnetic resonance (NMR) spectrum (Table 1) revealed six methyls [δ_H 1.65 (s, H_3-20), 1.03 (s, H_3-21), 1.10 (s, H_3-22), 1.05 (s, H_3-23), 1.58 (s, H_3-24), and 2.11 (s, H_3-32)] and five olefinic methines [δ_H 5.68 (m, H-3), 5.90 (d, *J* = 15.9 Hz, H-4), 6.14 (d, *J* = 2.3 Hz, H-28), 6.23 (d, *J* = 2.3 Hz, H-30), and 5.32 (s, H-18)]. The typical coupling constants (*J* = 2.3 Hz, H-28 and H-30) of aromatic protons indicated the presence of a 1,3,4,5-tetrasubstituted benzene ring. The ^{13}C NMR and heteronuclear single quantum correlation (HSQC) spectra displayed signals of 32 carbons, including six methyls, five methylenes, nine methines (two oxygenated and five olefinic), and twelve non-protonated carbons (six aliphatic, five olefinic, and one carboxyl). These NMR data suggested that **1** might be a meroterpenoid with a novel polycyclic backbone (Fig. 1).

The planar structure of **1** was determined primarily through analysis of 2D experimental data (Fig. 2). The ^{13}C NMR spectrum

* Corresponding author.
E-mail address: luoqi@smu.edu.cn (Q. Luo)
Δ These authors contributed equally to this work.

https://doi.org/10.1016/S1875-5364(26)61081-3

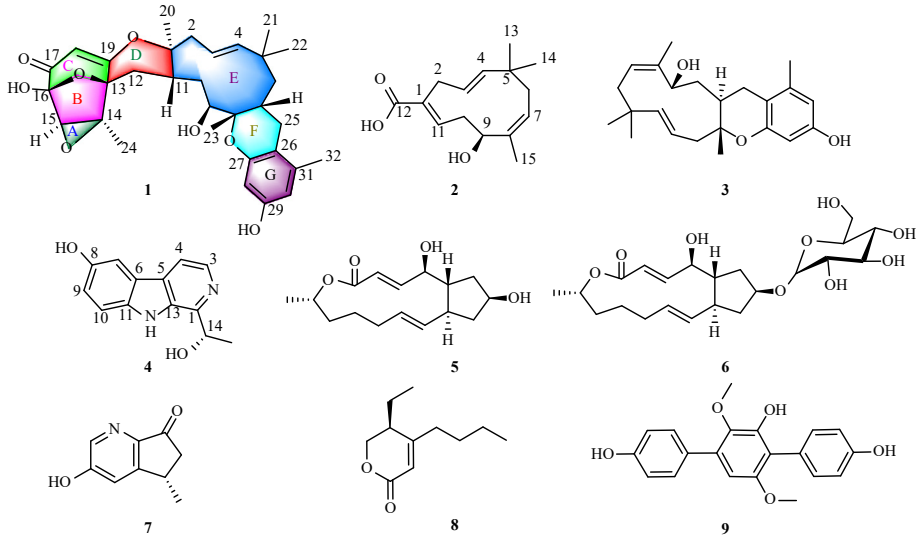

Fig. 1 The chemical structures of compounds **1**–**9**.

Table 1 ^{1}H (600 MHz) and ^{13}C NMR (150 MHz) data of **1** in methanol-d_4 (J in Hz).

No.	δ_H	δ_C	No.	δ_H	δ_C
1		90.4	16		102.2
2	Ha 2.69 overlap	48.0	17		196.3
	Hb 2.57 t-like (13.1)		18	5.32 s	105.0
3	5.67 m	125.4	19		182.0
4	5.90 d (15.9)	146.7	20	1.65 s	21.9
5		35.9	21	1.03 s	30.0
6	Ha 1.79 m	47.6	22	1.10 s	27.3
	Hb 0.77 dd (14.8, 5.0)		23	1.05 s	15.8
7	1.80 m	33.7	24	1.58 s	13.3
8		81.2	25	Ha 2.72 overlap	30.6
9	4.08 d (11.2)	71.9		Hb 2.28 d 15.7	
10	Ha 2.40 d-like (11.2)	32.9	26		111.2
	Hb 1.48 t-like (12.8)		27		155.5
11	2.16 m	44.0	28	6.14 d (2.3)	102.6
12	Ha 2.97 t (15.0)	32.1	29		157.2
	Hb 1.77 m		30	6.23 d (2.3)	110.5
13		82.8	31		139.9
14		68.6	32	2.11 s	19.4
15	3.43 s	61.1			

of **1** revealed two characteristic mid-field carbon signals at δ_C 68.6 (C-14) and 61.1 (C-15), indicating an oxirane subunit (ring A). The heteronuclear multiple bond correlation (HMBC) spectrum exhibited correlations between H-15 (δ_H 3.43)/C-13, C-14 (weak), C-16, and H_3-24 (δ_H 1.58)/C-13, C-14, C-15. Combined with the chemical shifts of C-13 (δ_C 82.8) and C-16 (δ_C 102.2), these data established the presence of a five-membered ring (ring B) containing a hydroxyl group at C-16. Furthermore, a six-membered rigid structure (ring C) with a bridgehead double bond (anti-Bredt system) was evidenced by the HMBCs of H-18/C-13, C-16, C-17 (weak), C-19, and their respective chemical shifts of C-17 (δ_C 196.3), C-18 (δ_C 105.0), C-19 (δ_C 182.0). These findings confirm a dioxatricyclo[3.3.1.0^{2,4}]nonane scaffold in nature

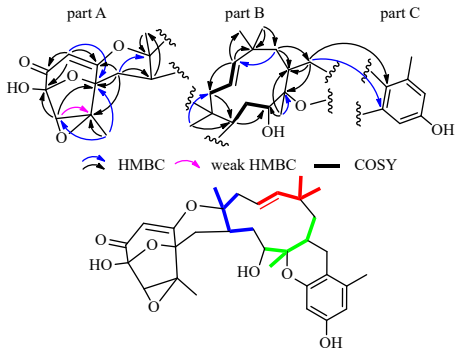

Fig. 2 Key ^{1}H–^{1}H COSY, and HMBCs of **1**. Blue, green, and red in **1** represent three independent isoprenyl moieties.

comprising rings A/B/C.

The methyl group at C-1 was confirmed through HMBCs of H_3-20 (δ_H 1.65) with C-1 (δ_C 90.4)/C-2 (δ_C 48.0)/C-11 (δ_C 44.0). The ^{1}H–^{1}H correlation spectroscopy (COSY) correlations of H-9/H-10/H-11 and HMBCs of Ha-2 (δ_H 2.69) with C-11 indicated a prenyl group (Fig. 2, blue line). A second prenyl moiety (red line) was identified through HMBCs of H-4 (δ_H 5.90) with C-5 (δ_C 35.9)/C-21 (δ_C 30.0)/C-22 (δ_C 27.3), Hb-6 (δ_H 0.77) with C-4 (δ_C 146.7)/C-7 (δ_C 33.7), and the ^{1}H–^{1}H COSY correlation of H-3/H-4. Additionally, HMBCs of H_3-23 (δ_H 1.05) with C-7 (δ_C 33.7)/C-8 (δ_C 81.2)/C-9 (δ_C 71.8) revealed the third prenyl subunit (Fig. 2, green line). These data indicated an eleven-membered ring composed of three isoprenyl moieties (part B). Further HMBC spectrum analysis revealed correlations of H-25 with C-6, C-7, C-8, C-26 (δ_C 111.2), C-27, along with chemical shifts of C-8 (δ_C 81.2) and C-27 (δ_C 155.0), indicating that the arene ring (Fig. 2, part C) was connected to C-8 *via* an oxygen bridge. This structural assignment was further supported by key rotating-frame Overhauser effect spectroscopy (ROESY) correlations of H-28/H_3-23.

In addition to an aromatic ring G, two double bonds, a carbonyl group, an oxirane subunit, a five-membered ring B, two six-membered rings C and F, and an eleven-membered large ring E accounting for eleven degrees of unsaturation, an additional ring is necessary to complete the structure of **1**. The presence of a six-membered ring D was confirmed by the ^{1}H–^{1}H correlations of H-11/H-12 and the HMBCs of H-12/C-1, C-11, C-13, C-14, C-19, and H-11/C-1, C-12, C-20, together with chemical shifts of C-1 (δ_C 90.4) and C-19 (δ_C 182.0). This evidence demonstrated the formation of a pyrano[3,2-*b*]pyran carbon framework sharing a com-

mon C-13–C-19 bond. Thus, the planar structure of **1** was established as depicted in Fig. 2.

The molecule contains nine chiral centers. The ROESY correlations of Ha-2 with H_3-20, Hb-2 with H-11, H-9 with H_3-20, Ha-10 with H_3-20, Ha-12 with H_3-20, Hb-10 with H_3-23, H-7 with H_3-23 (Fig. 3) indicated that H-9 and H_3-20 possessed α-configuration, while H-7, H-11, and H_3-23 exhibited β-configuration. The trisubstituted epoxide (ring A) in **1** necessitated that H-15 and H_3-24 were oriented in the same direction on the B ring, as supported by the key ROESY correlations between H-15 (δ_H 3.43)/H_3-24 (δ_H 1.58). Additional correlations between H_3-20 (δ_H 1.65)/H_3-24, Ha-12/H_3-20, Ha-12/H_3-24, and H_3-24/H-18 (δ_H 5.32), and the weak correlations between H-15 (δ_H 3.43)/H-18, H-18/H_3-20, indicated their spatial proximity. The conformationally rigid 6*H*-2,8a-epoxyoxireno[2',3':3,4]cyclohepta[1,2-*b*]pyran ring system (rings A–D) containing an unusual bridgehead double bond (anti-Bredt system) in **1** enabled the assignment of relative configurations at C-13 and C-16. The rigidity of the fused B/C rings, which are conformationally locked and incapable of ring inversion. The *E*-configuration of the Δ^3 double bond was determined by the coupling constant of H-4 (J = 15.9 Hz) and the ROESY correlation of H-4/Hb-2. Based on this evidence, the relative configuration at chiral carbons of **1** was definitively established as 1S^*,7R^*,8S^*,9S^*,11R^*,13R^*,14S^*,15R^*,16R^*.

Multiple solvent systems were employed in attempts to obtain crystals suitable for determining the absolute configuration of **1**. When crystallization proved challenging, electronic circular dichroism (ECD) calculations were conducted at the B3LYP/6-311 + G(2d, p) level with PCM in methanol to elucidate the absolute configurations of the chiral carbons. The analysis revealed that the weighted ECD spectrum of (1*S*,7*R*,8*S*,9*S*,11*R*,13*R*,14*S*,15*R*,16*R*)-**1** showed strong correlation with the experimental curve of **1** (Fig. 4), enabling definitive assignment of the absolute configurations of **1** as 1*S*,7*R*,8*S*,9*S*,11*R*,13*R*,14*S*,15*R*,16*R*. Given the unique carbon skeleton of **1**, additional ^{13}C NMR chemical shift calculations of (1*S*,7*R*,8*S*,9*S*,11*R*,13*R*,14*S*,15*R*,16*R*)-**1** were performed at the MPW1PW91/6-311 + G(2d, p) level with PCM in methanol [7]. The results demonstrated a correlation coefficient (R^2) of 0.998 65 between experimental and calculated data from linear regression analysis (Fig. 5), with mean absolute error (MAE) and corrected mean absolute error (CMAE) values of 2.8 and 1.5, respectively (Table S4, Supporting information), validating the structure of **1** determined through NMR experimental data. The density functional theory (DFT)-^{13}C NMR calculations thus provided additional confirmation of the 3/5/6/6/11/6/6 polycyclic backbone structure of **1**.

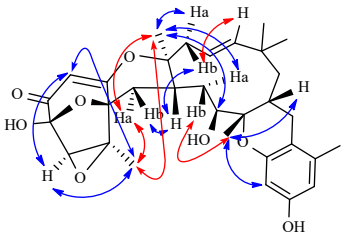

Fig. 3 Key ROESY correlations of **1**.

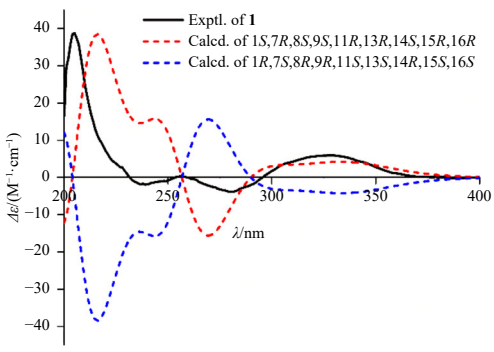

Fig. 4 Comparison of the calculated ECD spectra at the B3LYP/6-311 + G(2d, p) level with the experimental spectra of **1** (σ = 0.35 eV, shift = +5 nm) in MeOH.

Penicine A (**1**) represents the first known example of a meroterpenoid containing an unusual dioxatricyclo [3.3.1.0^{2,4}]nonane scaffold and a dioxaspiro[4.5]decane core. Natural products featuring anti-Bredt and bridgehead double bonds are rare, with only limited documented examples [7]. The discovery of **1** introduces a novel skeleton type of tropolonic meroterpenoids, warranting investigation of its potential biosynthetic pathway. Structural analysis of **1** (Scheme 1) reveals components including a sesquiterpenoid, a benzopyran, and a highly oxidized polycyclic core, suggesting biosynthetic derivation through combined polyketide and mevalonic acid pathways. A key precursor **C** likely originates from one acetyl-CoA and three malonyl-CoA units, condensed through the coordinated action of a non-reducing polyketide synthase (nrPKS), an FAD-dependent monooxygenase (FMO), and an α-ketoglutarate-dependent dioxygenase (KGD) [8, 9]. The corresponding alcohol, stipitol **D**, is generated *via* the enzymatic reduction of intermediate **C** by a short-chain dehydrogenase/reductase (SDR). The essential sesquiterpenoid **E** (10-hydroxy-8*Z*-humulene [10]) is biosynthesized from the C_{15} farnesyl diphosphate (FPP), which is formed through the canonical "head-to-tail" condensation of isopentenyl diphosphate (IPP) and dimethylallyl diphosphate (DMAPP), catalyzed by FPP synthase. This is followed by a "head-to-middle" cyclization of FPP mediated by a terpene cyclase, and a subsequent hydroxylation catalyzed by a cytochrome P450 monooxygenase [10]. A key intermediate **G** containing two cyclohepta[*b*]pyran subunits forms *via* tandem intermolecular Diels–Alder reactions between **E** and **D** [11]. Oxidation of **D** through a ring-opening-ring-closing mechanism yields intermediate **H** with a benzopyran motif. The final phase involves formation of the dioxatricyclo[3.3.1.0^{2,4}]nonane skeleton in **1** through oxidation processes and cyclization.

Penicine B (**2**) was isolated as a white powder. Its molecular formula of $C_{15}H_{22}O_3$ was determined by HR-ESI-MS m/z 249.1473 [M − H]$^-$ peak (Calcd. for $C_{15}H_{21}O_3$ 249.1496), indicating 5 degrees of unsaturation. The ^{1}H NMR spectrum (Table 1) revealed four olefinic protons [δ_H 5.22 (m, H-3), 5.28 (d, J = 16.0 Hz, H-4), 5.33 (m, H-7), and 7.16 (dd, J = 11.9, 5.8 Hz, H-11)], and three methyls [δ_H 1.01 (s, H_3-13), 1.07 (s, H_3-14), and 1.74 (s, H_3-15)]. The ^{13}C NMR spectrum exhibited signals of 15 carbons, including three methyls, three methylenes, five methines (four sp^2, one oxygenated), one aliphatic quaternary carbon, two olefinic non-protonated quaternary carbons, and one carboxyl group. These NMR data indicated that **2** is a sesquiterpenoid.

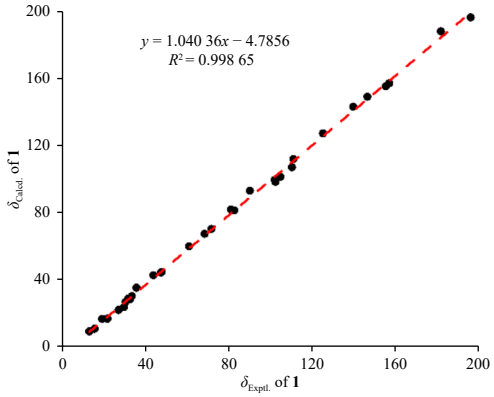

Fig. 5 Regression analysis of experimental versus calculated ^{13}C NMR chemical shifts of (1*S*,7*R*,8*S*,9*S*,11*R*,13*R*,14*S*,15*R*,16*R*)-**1** at the MPW1PW91-SCRF/6-311 + G(2d, p) level; linear fitting is shown as a line.

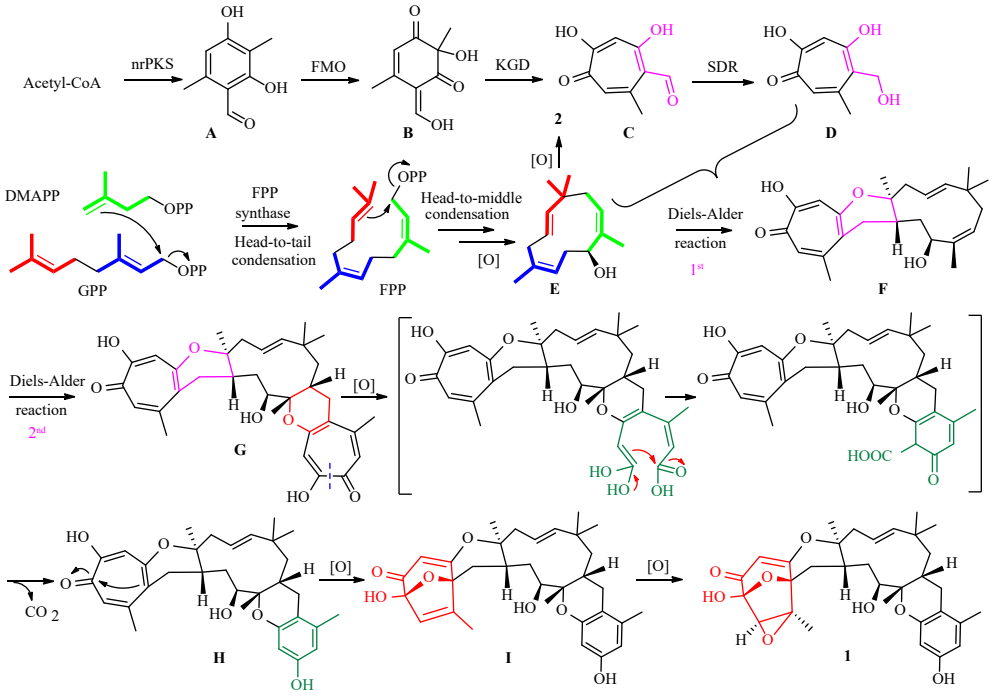

Scheme 1 Plausible pathway for the biogenesis of **1** and **2**.

The planar structure of **2** was established through analysis of 2D NMR spectral data (Fig. 6). The HMBC spectrum revealed correlations of H-11 with C-1 (δ_C 132.7)/C-2 (δ_C 31.4)/C-12 (δ_C 172.2), H-2 with C-1/C-4, and H_3-13 with C-4/C-5, and H_3-14 with C-5/C-6, indicating the presence of two isoprenyl moieties with a carboxyl group attached at C-1. Additionally, HMBCs of H-7 with C-6/C-9, H_3-15 with C-7/C-8/C-9, H-9 with C-10, and H-11 with C-10 indicated the presence of a third isoprenyl group containing a hydroxy group attached at C-9. These data confirmed the planar structure of **2** as illustrated (Fig. 6).

The relative configuration of **2** was determined through analysis of the NOESY spectrum (Fig. 6). ROESY correlations of H-2 with H-4, H-2 with H-10, and H_3-15 with H-7 indicated that two double bonds $\Delta^{3,4}$ and $\Delta^{1,11}$ possessed *E*-configuration, while the double bond $\Delta^{7,8}$ exhibited *Z*-form *β*-configuration. The absolute configuration of **2** was determined using ECD calculations (Tables S6–S9, Supporting information). The calculated weighted ECD spectrum of (9*S*)-**2** demonstrated good agreement with the experimental ECD spectrum of **2** (Fig. 7), enabling assignment of the absolute configuration at C-9. Based on the terpenoid biosynthetic pathway, **2** represents the oxidation product of key intermediate **E** (Scheme 1).

Penicine C (**4**) was isolated as a yellow powder with molecular formula $C_{13}H_{12}N_2O_2$, as determined by HR-ESI-MS and ^{13}C NMR data, indicating nine degrees of unsaturation. The ^1H and ^{13}C NMR spectral data of **4** (Table 2) exhibited close similarity to those of 1-(1-hydroxy)ethyl harmine analogue 3-3 [12], with the notable difference being the absence of a methoxyl group at C-9 and the presence of a hydroxyl group at C-8. This structural assignment was supported by key HMBCs of H-7 with C-6/C-8, and H-9 with C-10/C-11 (Fig. 6). Comparison of specific optical rotations of **4** {$[\alpha]_D^{25}$ +45.2 (*c* 0.05, MeOH)} with reported *β*-carboline alkaloid analogues [13] {cordysinin C, $[\alpha]_D^{25}$ −57.0 (*c* 0.05, MeOH), for 14*R* configuration; and cordysinin D, $[\alpha]_D^{25}$ +60.4 (*c* 0.05, MeOH), for 14*S* configuration} enabled assignment of the absolute configuration of **4** as 14*S*.

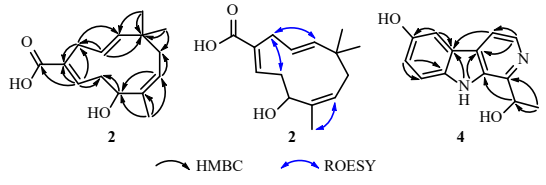

Fig. 6 Key HMBC and ROESY correlations of **2** and **4**.

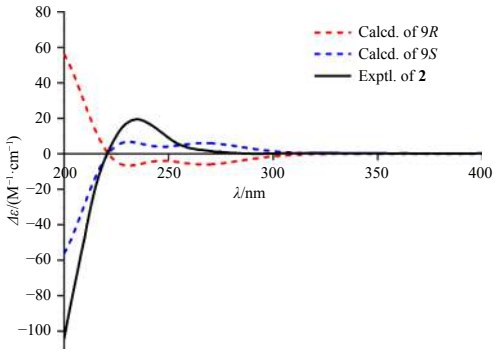

Fig. 7 Comparison of the calculated ECD spectra at the B3LYP/6-311 + G(2d, p) level with the experimental spectra of **2** (σ = 0.40 eV, shift = +0 nm) in MeOH.

Six known compounds were identified as pughiinin A (**3**) [6], brefeldin A (**5**) [14], 7-*O*-*α*-D-glucosyl-brefeldin A (**6**) [15], 3-hydroxy-5-methyl-5,6-dihydro-7*H*-cyclopenta[*b*]pyridin-7-one (**7**) [16], 4-butyl-5-ethyl-3,4-dihydropyran-2-one (**8**) [17], and terphenyllin (**9**) [18], respectively, through comparison of their NMR spectral data with literature values.

Fibronectin (FN), a principal non-collagenous glycoprotein in the extracellular matrix (ECM) and basement membrane, facilitates the differentiation of fibroblasts to myofibroblasts, which may represent a critical mechanism in the pathogenesis of tubulointerstitial fibrosis [19]. *In vivo*, the classical fibrosis marker FN exhibited continuous elevation over time in the irreversible UUO model. In the activity evaluation experiment, compounds **1**–**9** were evaluated for their potential antifibrotic activity in TGF-β1-induced human renal proximal tubular epithelial cells (HK-2) using Western blot analysis. The results demonstrated that penicine A (**1**, 40 μmol·L^{-1}) and pughiinin A (**3**, 20 μmol·L^{-1}) significantly reduced the overexpression of FN, indicating that meroterpenoids **1** and **3** might serve as potent inhibitors of renal

Table 2 ^{1}H (600 MHz) and ^{13}C NMR (150 MHz) data of **2** and **4** (*J* in Hz).

No.	**2**[a]		No.	**4**[b]	
	δ_H	δ_C		δ_H	δ_C
1		132.7	1		148.5
2	Ha 3.36 dd (13.1, 2.6)	31.4	3	8.13 d (5.2)	135.8
	Hb 2.79 dd (13.1, 9.9)		4	7.86 d (5.2)	113.5
3	5.22 m	124.3	5		127.9
4	5.28 d (16.0)	143.1	6		121.1
5		38.5	7	7.49 d (8.7)	112.9
6	Ha 2.17 t (11.7)	43.8	8		150.7
	Hb 1.80 dd (12.9, 6.7)		9	7.03 dd (8.7, 2.1)	118.0
7	5.33 m	122.6	10	7.46 d (2.1)	105.3
8		141.7	11		134.7
9	4.31 d (8.6)	71.7	12	10.9 s	
10	Ha 2.42 t-like (12.4)	36.6	13		132.9
	Hb 2.27 m		14	5.16 dd (13.0, 6.5)	69.2
11	7.16 dd (11.9, 5.8)	143.5	15	1.52 d (6.6)	22.9
12		172.2			
13	1.01 s	27.1			
14	1.07 s	28.4			
15	1.74 s	17.2			

[a] recorded in methanol-d_4; [b] recorded in DMSO-d_6.

fibrosis (Fig. 8).

3. Conclusions

In summary, a novel meroterpenoid **1** featuring a 3/5/6/6/11/6/6 polycyclic backbone, along with two new metabolites, penicines B (**2**) and C (**4**), and six known compounds, were isolated from the mangrove rhizosphere soil-derived fungus *Penicillium brefeldianum* SMU03. Notably, compound **1** contains a naturally rare dioxatricyclo[3.3.1.0^{2,4}]nonane scaffold, a dioxaspiro [4.5]decane core, and an unusual bridgehead double bond (anti-Bredt system). Its proposed biosynthetic route correlates with tandem intermolecular [4 + 2] cycloaddition reactions. A detailed structural comparison between compounds **1** and **2** reveals that compound **2** represents a significant structural component of compound **1**, supporting the formation of **1** through two distinct biosynthetic pathways. Furthermore, biological evaluation demonstrated that tropolonic meroterpenoids **1** and **3** show promise as novel antifibrotic agents, highlighting the potential of penicillia-associated fungi in discovering natural products with novel skeletal structures and pharmacological activities.

4. Experimental

4.1. General experimental procedures

1D and 2D NMR spectra were obtained using a Bruker AVANCE III HD 600 MHz NMR spectrometer (Bruker) with TMS as an internal standard. Structural assignments were determined using additional information from COSY, HSQC, HMBC, and ROESY experimental data. Optical rotations were measured on an Autopol-I digital polarimeter (New Jersey, USA). UV and CD spectra were recorded with a Chirascan circular dichroism spectrometer (Applied Photophysics Ltd., Surrey, UK). HR-ESI-MS was conducted using a Sciex X500R QTOF MS spectrometer with a Waters Acquity UPLC BEH C_{18} column (2.1 mm × 100 mm, 1.7 μm). Semi-preparative high-performance liquid chromatography (HPLC) was performed using a Shimadzu LC-20AT chromatograph (Shenshu Scientific, Tokyo, Japan) with a YMC-Pack ODS-A column (250 mm × 10 mm, S-5 μm, YMC Co., Ltd., Kyoto, Japan). Silica gel (200–300 mesh, Qingdao Haiyang Chemical Co., Ltd.) and Sephadex LH-20 (Amersham Pharmacia, Sweden) were utilized for column chromatography.

4.2. Fungal materials

The Fungus *Penicillium brefeldianum* SMU03 (GenBank:

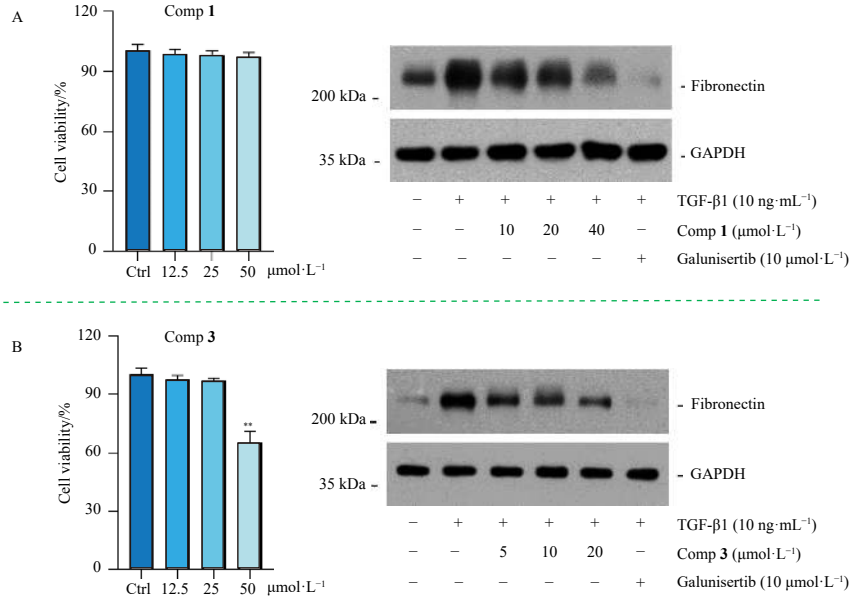

Fig. 8 HK-2 cell proliferation in response to meroterpenoids **1** and **3** at 12.5, 25, and 50 μmol·L^{-1} by CCK-8 assay. Data were expressed as mean ± SEM (n = 3), $^{**}P < 0.01$ *vs* Ctrl alone. Meroterpenoids **1** and **3** attenuate renal fibrosis in TGF-β1-induced HK-2 cells. HK-2 cells were incubated with TGF-β1 (10 ng·mL^{-1}) for 48 h in the absence or presence of different concentrations of **1** or **3**. The protein level of FN in HK-2 was determined by Western blot, and GAPDH was used as a control. Galunisertib (purchased from MCE) was used as a positive control.

OR453083) was isolated from mangrove soil collected from Wetland Parks of Huiyang, Guangzhou, China, and identified through ITS sequence analysis. The strain was deposited at the Syndrome Laboratory of Integrated Chinese and Western Medicine, Southern Medical University, China.

4.3. Fermentation and extraction

The mangrove rhizosphere soil-derived fungus *Penicillium brefeldianum* SMU03 was initially cultivated in 3 × 15 mL test tubes, each containing 4 mL of potato dextrose (PD) medium (2% glucose and 20% potato extract). The cultures were incubated on a thermostatic shaker at 200 r·min^{-1} for 3 d at 28 °C. The resulting mycelial biomass was then transferred into 7 × 1000 mL Erlenmeyer flasks, each containing 300 mL of medium supplemented with 3% malt extract, and subjected to further fermentation under shaking conditions (180 r·min^{-1}) for 3 d at 30 °C. Then, 6–10 mL aliquots of the mycelia suspension were inoculated into 230 × 750 mL hexagonal flasks, each containing 300 mL of 1# medium (2% maltose, 2% sorbitol, 1% monosodium glutamate, 0.3% yeast, 0.3% salt, 0.05% KH_2PO_4, 0.05% tryptophan, 0.03% $MgSO_4$•$7H_2O$). The cultures were then incubated under static conditions at 26 °C for 30 d.

Subsequently, the mycelia of *Penicillium brefeldianum* SMU03 were extracted five times with methanol (2 × 30 L) at room temperature to obtain crude extract, which was suspended in water and extracted with ethyl acetate (three times). The broth was directly extracted with ethyl acetate (three times). Finally, a total EtOAc soluble extract was obtained.

4.4. Isolation and purification

The crude extracts (11.2 g) were fractionated by medium-pressure column using stepped gradient elution with CH_2Cl_2/MeOH (*V/V*, 100∶0, 95∶5, 90∶10, 80∶20, 70∶30, 60∶40, 50∶50; each gradient using 1.5 L elution mixture) to obtain six fractions (Fr.1–Fr.6) according to TLC. Fr.1 (3.0 g) was fractionated by medium-pressure column using stepped gradient elution with petroleum ether/EtOAc (*V/V*, 100∶0, 30∶1, 20∶1, 15∶1, 10∶1, each gradient using 0.5 L elution mixture) to yield nine fractions (Fr.1.1–Fr.1.9). Among these, Fr.1.2 was purified by semi-preparative HPLC eluting with MeOH/H_2O/TFA (*V/V/V*, 94∶6∶0.01; flow rate: 3.0 mL·min^{-1}) to yield **8** (34.6 mg, t_R 20.9 min).

Fr.2 (2.7 g) was fractionated into six portions (Fr.2.1–Fr.2.6) using Sephadex LH-20 with MeOH as eluent. Fr.2.1 (0.1 g) underwent purification by semi-preparative HPLC using MeOH/H_2O/TFA (*V/V/V*, 96∶4∶0.01; flow rate: 2.5 mL·min^{-1}) to yield **9** (1.6 mg, t_R 9.0 min). Fr.2.3 (0.3 g) was purified *via* semi-preparative HPLC using MeOH/H_2O/TFA (*V/V/V*, 72∶28∶0.01; flow rate: 3.0 mL·min^{-1}) to obtain **1** (5.0 mg, t_R 19.8 min), **2** (1.9 mg, t_R 13.2 min), **3** (11.2 mg, t_R 15.1 min), and **7** (2.8 mg, t_R 6.0 min).

Fr.3 (0.47 g) underwent separation using Sephadex LH-20 with CH_3OH as eluent, yielding five fractions (Fr.3.1–Fr.3.5). Fr.3.2 (0.28 g) was subsequently purified by semi-preparative HPLC using MeOH/H_2O/TFA (*V/V/V*, 68∶32∶0.01; flow rate: 2.5 mL·mL^{-1}) to produce **5** (55.0 mg, t_R 13.5 min). Fr.4 (1.2 g) was separated using Sephadex LH-20 with CH_3OH as eluent into seven fractions (Fr.4.1–Fr.4.7). Fr.4.2 (0.2 g) underwent separation by semi-preparative HPLC using MeOH/H_2O/TFA (*V/V/V*, 68∶32∶0.01, flow rate: 2.5 mL·mL^{-1}) to yield **6** (8.4 mg, t_R 10.8 min). Fr.4.3 (0.45 g) was isolated using semi-preparative HPLC eluting with CH_3CN/H_2O/TFA (*V/V/V*, 15∶85∶0.04, flow rate: 2.5 mL·mL^{-1}) to obtain **4** (1.4 mg, t_R 14.8 min)

Penicine A (**1**): white powder; $[\alpha]_D^{25}$ +137.3 (*c* 0.1, MeOH); UV (MeOH) λ_{max} (log ε): 204 (1.59), 225 (1.09), 243 (0.86), 260 (1.06) nm; ECD (0.045 mmol·L^{-1}, MeOH) $\Delta\varepsilon_{205}$ +38.8, $\Delta\varepsilon_{239}$ −1.92, $\Delta\varepsilon_{281}$ −3.81, $\Delta\varepsilon_{327}$ +5.95; HR-ESI-MS (ESI-TOF) *m/z*: [M + H]$^+$ Calcd. for $C_{32}H_{41}O_8$ 553.2796; Found 553.2797. ^{1}H and ^{13}C NMR data, see Table 1.

Penicine B (**2**): white powder; $[\alpha]_D^{25}$ −49.6 (*c* 0.05, MeOH); UV (MeOH) λ_{max} (log ε): 200 (4.15), 225 (3.78) nm; ECD (0.01 mmol·L^{-1}, MeOH) $\Delta\varepsilon_{235}$ +19.76; HR-ESI-MS: *m/z* 249.1473 [M − H]$^-$ (Calcd. for $C_{15}H_{21}O_3$, 249.1496); ^{1}H and ^{13}C NMR data, see Table 2.

Penicine C (**4**): yellow powder; $[\alpha]_D^{25}$ +45.2 (*c* 0.05, MeOH); UV (MeOH) λ_{max} (log ε): 231 (4.12), 297 (3.82) nm; HR-ESI-MS: *m/z* 227.0815 [M − H]$^-$ (Calcd. for $C_{13}H_{11}N_2O_2$, 227.0826); ^{1}H and ^{13}C NMR data, see Table 2.

4.5. Kidney fibrosis activity methods

4.5.1. Cell culture

HK-2 human renal proximal tubular epithelial cells (provided by Procell Life Science & Technology Co., Ltd.) were maintained in DMEM/F12 (C11330500BT, Gibco, Waltham, MA, USA) supplemented with 10% fetal bovine serum (FBS, RY-F22, Royacel, Lanzhou, China), 100 U·mL^{-1} penicillin, and 100 μg·mL^{-1} streptomycin at 37 °C in a humidified environment containing 5% CO_2.

4.5.2. Cell counting kit-8 (CCK-8) assay for cell viability assessment

HK-2 cells in logarithmic phase were seeded at 8000 cells per well in 96-well flat-bottomed microtiter plates. Cells were treated with varying concentrations of compounds **1**–**9**. Following 48 h incubation, 10 μL of CCK-8 was added to each well and incubated at 37 °C for 2 h. The absorbance was measured at 450 nm using a microplate reader.

4.5.3. Western blot analysis

HK-2 cells were treated with TGF-β1 (10 ng·mL^{-1}, 100-21, Peprotech, Cranbury, NJ, USA) for 48 h with or without compounds. Cell lysates were prepared using RIPA buffer (G2002, Servicebio, Wuhan, China) containing 1× protease inhibitor cocktail (20124E03, Yeasen Biotech, Mannheim, Germany) and 0.1 mmol·L^{-1} PMSF. Protein quantification was performed using the BCA assay (G2026, Servicebio, Wuhan, China). Equal protein amounts were separated by SDS-PAGE and transferred to NC membranes (Millipore, Darmstadt, Germany). The membranes were blocked with 5% BSA and incubated with primary antibodies overnight at 4 °C, followed by horseradish peroxidase (HRP)-conjugated secondary antibody incubation at room temperature for 1 h. Protein bands were visualized using the ECL kit (P1010, Applygen Technologies Inc., Beijing, China). Primary antibodies included anti-FN polyclonal antibody (#15613-1-AP, Proteintech, Wuhan Sanying, Wuhan, China) and anti-GAPDH monoclonal antibody (#60004-1-Ig, Proteintech, Wuhan Sanying, Wuhan, China).

4.6. ECD and ^{13}C NMR calculation methods

Molecular Merck force field (MMFF) and DFT and time-dependent density functional theory (TDDFT) calculations were conducted using Spartan'14 software package (Wavefunction Inc., Irvine, CA, USA) and Gaussian 16 program package [20], respectively. The detailed ECD and ^{13}C NMR calculation procedures followed previously reported methods [21]. The shielding constant calculation for TMS yielded σ_{ref} = 187.8170.

Funding

This work was supported by the National Natural Science Foundation of China (Nos. 82104039 and 82404471), Guangdong Science Foundation for Young Top-Notch Talent of Zhu-Jiang Talent Plan (No. 0920220225), Guangdong Basic and Ap-

plied Basic Research Foundation (Nos. 2023B1515120053 and 2022A1515111026), and Guangzhou Municipal Science and Technology Bureau Foundation (No. 2024A04J2704).

Supporting information

The Supporting information of 1D and 2D NMR spectra, HR-ESI-MS and UV spectra of new compounds **1**, **2**, and **4**, ECD or ^{13}C NMR calculations of compounds **1** and **2** can be requested by sending E-mail to the corresponding author.

Declaration of competing interest

The authors declare that they have no known competing financial interests or personal relationships that could have appeared to influence the work reported in this paper.

References

1 Cheng X, Liang X, Zheng ZH, et al. Penicimeroterpenoids A–C, meroterpenoids with rearrangement skeletons from the marine-derived fungus *Penicillium* sp. SCSIO 41512. *Org Lett*. 2020;22(16):6330-6333. https://doi.org/10.1021/acs.orglett.0c02160.
2 Xia GY, Wang LY, Zhang JF, et al. Three new polyoxygenated bergamotanes from the endophytic fungus *Penicillium purpurogenum* IMM 003 and their inhibitory activity against pancreatic lipase. *Chin J Nat Med*. 2020;18(1):75-80. https://doi.org/10.1016/S1875-5364(20)30007-8.
3 Chen XH, Zhou GL, Sun CX, et al. Penicacids E–G, three new mycophenolic acid derivatives from the marine-derived fungus *Penicillium parvum* HDN17-478. *Chin J Nat Med*. 2020;18(11):850-854. https://doi.org/10.1016/S1875-5364(20)60027-9.
4 Yan YM, Ai J, Zhou LL, et al. Lingzhiols, unprecedented rotary door-shaped meroterpenoids as potent and selective inhibitors of p-Smad3 from *Ganoderma lucidum*. *Org Lett*. 2013;15(21):5488-5491. https://doi.org/10.1021/ol4026364.
5 Luo Q, Di L, Dai WF, et al. Applanatumin A, a new dimeric meroterpenoid from *Ganoderma applanatum* that displays potent antifibrotic activity. *Org Lett*. 2015;17(5):1110-1113. https://doi.org/10.1021/ol503610b.
6 Pittayakhajonwut P, Theerasilp M, Kongsaeree P, et al. Pughiinin A, a sesquiterpene from the fungus *Kionochaeta pughii* BCC 3878. *Planta Med*. 2002;68(11):1017-1019. https://doi.org/10.1055/s-2002-35653.
7 Cheng X, Ma FP, Yan YM, et al. Aspertaichunol A, an immunomodulatory polyketide with an uncommon scaffold from the insect-derived endophytic *Aspergillus taichungensis* SMU01. *Org Lett*. 2022;24(40):7405-7409. https://doi.org/10.1021/acs.orglett.2c02978.
8 Schotte C, Li L, Wibberg D, et al. Synthetic biology driven biosynthesis of unnatural tropolone sesquiterpenoids. *Angew Chem Int Ed*. 2020;59(52):23870-23878. https://doi.org/10.1002/anie.202009914.
9 Zhang JY, Liu L, Wang B, et al. Phomanolides A and B from the fungus *Phoma* sp.: meroterpenoids derived from a putative tropolonic sesquiterpene *via* hetero-Diels-Alder reactions. *J Nat Prod*. 2015;78(12):3058-3066. https://doi.org/10.1021/acs.jnatprod.5b00969.
10 Liu JW, Lu JY, Zhang C, et al. Tandem intermolecular [4 + 2] cyclo additions are catalysed by glycosylated enzymes for natural product biosynthesis. *Nat Chem*. 2023;15(8):1083-1090. https://doi.org/10.1038/s41557-023-01260-8.
11 Chen QB, Gao J, Jamieson C, et al. Enzymatic itermolecular hetero-Diels-Alder reaction in the biosynthesis of tropolonic sesquiterpenes. *J Am Chem Soc*. 2019;141(36):4052-14056. https://doi.org/10.1021/jacs.9b06592.
12 Kumar K, Wang P, Sanchez R, et al. Development of kinase-selective, harmine-based DYRK1A inhibitors that induce pancreatic human *β*-cell proliferation. *J Med Chem*. 2018;61(17):7687-7699. https://doi.org/10.1021/acs.jmedchem.8b00658.
13 Yang ML, Kuo PC, Hwang TL, et al. Anti-inflammatory principles from *Cordyceps sinensis*. *J Nat Prod*. 2011;74(9):1996-2000. https://doi.org/10.1021/np100902f.
14 Chinworrungsee M, Wiyakrutta S, Sriubolmas N, et al. Cytotoxic activities of trichothecenes isolated from an endophytic fungus belonging to order hypocreales. *Arch Pharm Res*. 2008;31(5):611-616. https://doi.org/10.1007/s12272-001-1201-x.
15 Zheng YG, Wang YJ, Wu ZX, et al. Preparation and application of glycosylated derivative of brefeldin A. China: CN103739644A, 2014.
16 Peng XP, Wang Y, Liu PP, et al. Aromatic compounds from the halotolerant fungal strain of *Wallemia sebi* PXP-89 in a hypersaline medium. *Arch Pharm Res*. 2011;34(6):907-912. https://doi.org/10.1007/s12272-011-0607-0.
17 Caliskan H, Ozer M, Sabudak T, et al. A new pyran derivative analog from the whole plant of *Cirsium italicum*. *J Asian Nat Prod Res*. 2021;23(10):1009-1014. https://doi.org/10.1080/10286020.2020.1816977.
18 Ye WX, Zhao MR, Wang L, et al. Isolation, identification, and bioactive metabolites of coral-derived fungus *Aspergillus* sp. SCSIO 40435 from the South China Sea. *Acta Microbiol Sin*. 2022;62:1819-1831. https://doi.org/10.13343/j.cnki.wsxb.20210568.
19 Luo Q, Tian L, Di L, et al. (±)-Sinensilactam A, a pair of rare hybrid metabolites with potent Smad3 phosphorylation inhibition from *Ganoderma sinensis*. *Org Lett*. 2015;17:1565-1568. https://doi.org/10.1021/acs.orglett.5b00448.
20 Frisch MJ, Trucks GW, Schlegel HB, et al. Gaussian 16, revision C.01. Gaussian, Inc.: Wallingford CT, 2010.
21 Luo Q, Wei XY, Yang J, et al. Spiro meroterpenoids from *Ganoderma applanatum*. *J Nat Prod*. 2017;80(1):61-70. https://doi.org/10.1021/acs.jnatprod.6b00431.